

The Measurement of the Number of Light Neutrino Species at LEP

Salvatore Mele

*CERN, CH-1211 Geneva 23, Switzerland
salvatore.mele@cern.ch*

Within weeks of the start of the data taking at the LEP accelerator, the ALEPH, DELPHI, L3 and OPAL experiments were able to confirm the existence of just three light neutrino species. This measurement relies on the Standard Model relation between the ‘invisible’ width of the Z-boson and the cross-sections for Z-boson production and subsequent decay into hadrons.

The full data sample collected by the experiments at and around the Z-boson resonance allows a high-precision measurement of the number of light neutrino species as 2.9840 ± 0.0082 . The uncertainty is mostly due to the understanding of the low-angle Bhabha scattering process used to determine the experimental luminosity.

This result is independently confirmed by the elegant direct observation of the $e^-e^+ \rightarrow \nu\bar{\nu}\gamma$ process, through the detection of an initial-state-radiation photon in otherwise empty detectors.

This result confirms expectations from the existence of three charged leptons species, and contributes to the fields of astrophysics and cosmology. Alongside other LEP achievements, the precision of this result is a testament to the global cooperation underpinning CERN’s fourth decade. LEP saw the onset of large-scale collaboration across experiments totaling over 2000 scientists, together with a strong partnership within the wider high-energy physics community: from accelerator operations to the understanding of theoretical processes.

1. Introduction

The inception, design and approval of the LEP program at CERN, and the subsequent monumental construction of the accelerator and the detectors, represents a watershed in the history of the laboratory. The scientific, organizational and sociological challenges are described first hand in Ref. 1. The largest scientific instrument ever built, LEP was designed to push the frontiers of knowledge and understand the Standard Model of the electroweak interactions, with high-precision measurements of the properties of the recently discovered Z and W bosons.

One in five Z bosons produced at LEP decays into a “light neutrino”, that is a neutrino whose mass is less than half the Z-boson mass. The Standard Model relation between this decay width and the cross-section for Z-boson production and subsequent decay into hadrons makes it possible to infer the number of light neutrino species, N_ν .²

Table 1 Early measurements of the number of light neutrino species by each of the four LEP experiments, and their average. Uncertainties are dominated by the scale of the observed Z-boson production cross-section.

Experiment	N_ν	Reference
ALEPH	3.27 ± 0.30	4
DELPHI	2.4 ± 0.6	5
L3	3.42 ± 0.48	6
OPAL	3.1 ± 0.4	7
Average	3.10 ± 0.04	8

The first beams circulated in the LEP accelerator on 14th July 1989. The first data-taking campaign was at centre-of-mass energies around 90 GeV, compatible with the mass^a of the Z boson measured by the UA1 and UA2 experiments.³ By mid October 1989, the four LEP experiments, ALEPH, DELPHI, L3 and OPAL, had already published their first articles describing the Z boson properties.⁴⁻⁷ As listed in Table 1, these early observations already allowed to constrain N_ν to be around 3.

This article describes in details the measurement of N_ν in the context of the LEP high-precision physics program. Beyond the physics achievement, this measurement gives an insight on what made the LEP program so successful: a unique combination of exceptional accelerator performance, creative technological achievements in building and operating the detectors, and unprecedented cooperation with the theoretical physics community. These aspects set the scene for turning an important page in the history of CERN, then in its fourth decade. Such an enhanced culture of collaboration would usher the LHC era in CERN's fifth and sixth decades, as a worldwide hub of cooperation and creativity.

The structure of this article is the following. After this introduction, Section 2 recalls the principles of the indirect measurement of N_ν , including some concepts of the Standard Model of the electroweak interactions. Section 3 describes the experimental approach, including a broad-brush description of the LEP detectors, and presents the results of the measurement and a discussion of the uncertainties. Section 4 highlights a complementary direct measurement of N_ν through the detection of spectacular events with a single photon in otherwise empty detectors. Section 5 offers some concluding considerations.

2. Theoretical Principles

A cornerstone of the LEP physics program is the study of the Z-boson “lineshape”. This encompasses the measurement of parameters of the Standard Model of the

^aWe assume $h = 2\pi$ and $c = 1$, while using the factor 0.389 to convert GeV² into mb⁻¹.

electroweak interactions, and the proof of its internal consistency, through the study of physical observables describing Z-boson production and decay. Among these observables, the ‘invisible’ width of the Z-boson is related to its decay into neutrinos and gives access to N_ν . This section presents the physical observables leading to the measurement of N_ν and some key theoretical assumptions.

2.1. The width of the Z boson

The width of the Z boson is defined as

$$\Gamma_Z = \Gamma_{ee} + \Gamma_{\mu\mu} + \Gamma_{\tau\tau} + \Gamma_{\text{had}} + N_\nu \Gamma_{\nu\nu}, \quad (1)$$

where the first three terms are the widths of decays into electrons, muons and taus, respectively. Γ_{had} is the sum of the widths of decays into u, d, s, c and b quarks and $\Gamma_{\nu\nu}$ the width of decays into neutrinos. The simultaneous measurement of Γ_Z , and of observables related to the hadronic and leptonic widths of the Z boson, allows one to determine N_ν .²

The partial decay widths of the Z boson into each fermion pair are related to the Z-boson couplings and to Standard Model parameters as:^{9–11}

$$\Gamma_{f\bar{f}} = N_c^f \frac{G_F m_Z^3}{6\sqrt{2}\pi} \left(|G_{Af}|^2 R_{Af} + |G_{Vf}|^2 R_{Vf} \right) + \Delta_{\text{ew/QCD}} \quad (2)$$

where N_c^f is the number of colours (three for quarks and one for leptons), G_F is the Fermi constant determined from muon decay,¹² R_{Af} and R_{Vf} factorise final-state QED and QCD corrections and contributions from non-zero fermion masses to the axial and vector terms, respectively, $\Delta_{\text{ew/QCD}}$ accounts for non-factorisable electroweak and QCD corrections, and G_{Af} and G_{Vf} are the axial and vector effective couplings of the Z-boson to fermions, written as¹³

$$G_{Af} = \sqrt{R_f} T_3^f, \quad (3)$$

$$G_{Vf} = \sqrt{R_f} (T_3^f - 2Q_f K_f \sin \theta_W). \quad (4)$$

The form factors R_f and K_f absorb the overall scale of the coupling and the on-shell corrections to the electroweak mixing angle, θ_W , Q_f and T_3^f are the electric charge and the third component of weak isospin of the fermion, respectively.

2.2. Experimental observables

Four experimental observables describe the total hadronic and leptonic cross section around the Z-boson resonance, and connect N_ν to the Z-boson lineshape:

- (1) the mass of the Z boson, m_Z ;
- (2) the width of the Z boson, Γ_Z ;

(3) the hadronic pole cross-section

$$\sigma_{\text{had}}^0 = \frac{12\pi \Gamma_{ee} \Gamma_{\text{had}}}{m_Z^2 \Gamma_Z^2}; \quad (5)$$

(4) the ratio of the Z-boson partial decay widths into hadrons and massless leptons, Γ_{ll} , assuming lepton universality:

$$R_l^0 = \frac{\Gamma_{\text{had}}}{\Gamma_{ll}}. \quad (6)$$

The non-negligible tau mass is accounted for as $\Gamma_{ll} = \delta_\tau \Gamma_{\tau\tau}$, with $\delta_\tau = -0.23\%$. A fifth experimental observable, less important for the N_ν determination, is the lepton forward-backward asymmetry, again assuming lepton universality:

(5) $A_{\text{FB}}^{0,1}$,

which is defined as the asymmetry at the Z-boson pole of the cross-sections for final state leptons emitted in the forward (i.e. the negative-charged lepton ‘continuing’ along the direction of the incoming electron) or backward direction, according to the general formula $A_{\text{FB}} = (\sigma_{\text{F}} - \sigma_{\text{B}})/(\sigma_{\text{F}} + \sigma_{\text{B}})$.

2.3. Sensitivity to N_ν

A key experimental observable directly related to N_ν is

$$R_{\text{inv}}^0 = \frac{\Gamma_{\text{inv}}}{\Gamma_{ll}} = N_\nu \left(\frac{\Gamma_{\nu\nu}}{\Gamma_{ll}} \right). \quad (7)$$

The asset of R_{inv}^0 is that uncertainties of experimental and theoretical nature are well-controlled in the ration of the Z-boson widths.

The combination of Eqs. (2) and (5) allows to write R_{inv}^0 as

$$R_{\text{inv}}^0 = \left(\frac{12\pi R_l^0}{\sigma_{\text{had}}^0 m_Z^2} \right)^{\frac{1}{2}} - R_l^0 - (3 + \delta_\tau), \quad (8)$$

which expresses, together with Eq. (7), the relation between N_ν and the hadronic pole cross-section. This dependency drives the determination of N_ν and is graphically displayed in Fig. 1, which compares the measured hadron production cross-section around the Z-boson resonance with predictions for two, three and four light neutrino species. The curves in Fig. 1 allow to visualise the enormous statistical sensitivity of LEP data to N_ν .

It is important to summarise the assumptions made in describing the dependence of N_ν on the physical observables at LEP: lepton universality holds; Z bosons only decay to known fermions; neutrino masses are negligible; and Z-boson couplings to neutrinos are described by the Standard Model.

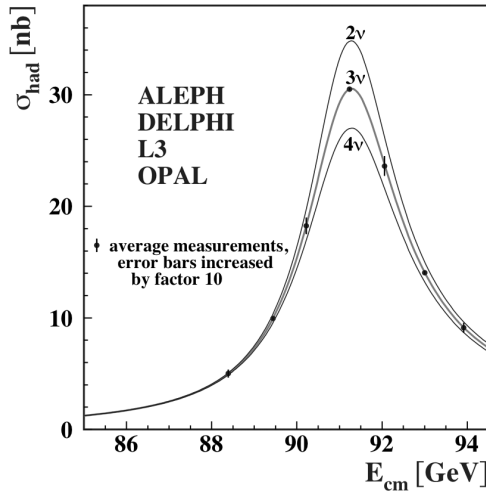


Fig. 1. Measurement of the hadron production cross-section as a function of the LEP centre-of-mass energy around the Z-boson resonance. Combined results from the four LEP experiments are presented. Curves represent the predictions for two, three and four neutrino species. To further convey the high sensitivity of the measurement, uncertainties are magnified tenfold.¹⁴

3. Experimental Measurement

The LEP accelerator and the LEP detectors were unprecedented in their size and complexity. This Section gives a succinct description of how the challenges of high-precision Z-boson detection guided detector design. After recalling the data sample, the measurements of the key observables leading to N_ν are presented, together with the final result, and crucial uncertainties are discussed.

3.1. Detection of Z-boson decays

The design of the four LEP experiments^{15–18} was optimised to detect Z-boson decays with high efficiency, within the available budgetary, technological and physical constraints. Teams of several hundred scientists, technicians and engineers designed, prototyped, built and assembled sophisticated apparatuses with dimensions exceeding 10 metres in diameter and length, and weighting several thousand tons. While the basic design principles of the detectors were similar, the choices of particular technologies in some sub-detectors were markedly different and would eventually contribute to reduce combined systematical uncertainties.

Figure 2 presents a cut-away three-dimensional view of the four detectors. All are radially and forward-backward symmetric. The common part of the design is the succession of sub-detectors, moving outwards from the beam axis: tracking chambers, surrounded by calorimeters and bending magnets, with muon spectrometers as the outmost layer. The exception is the L3 detector where the

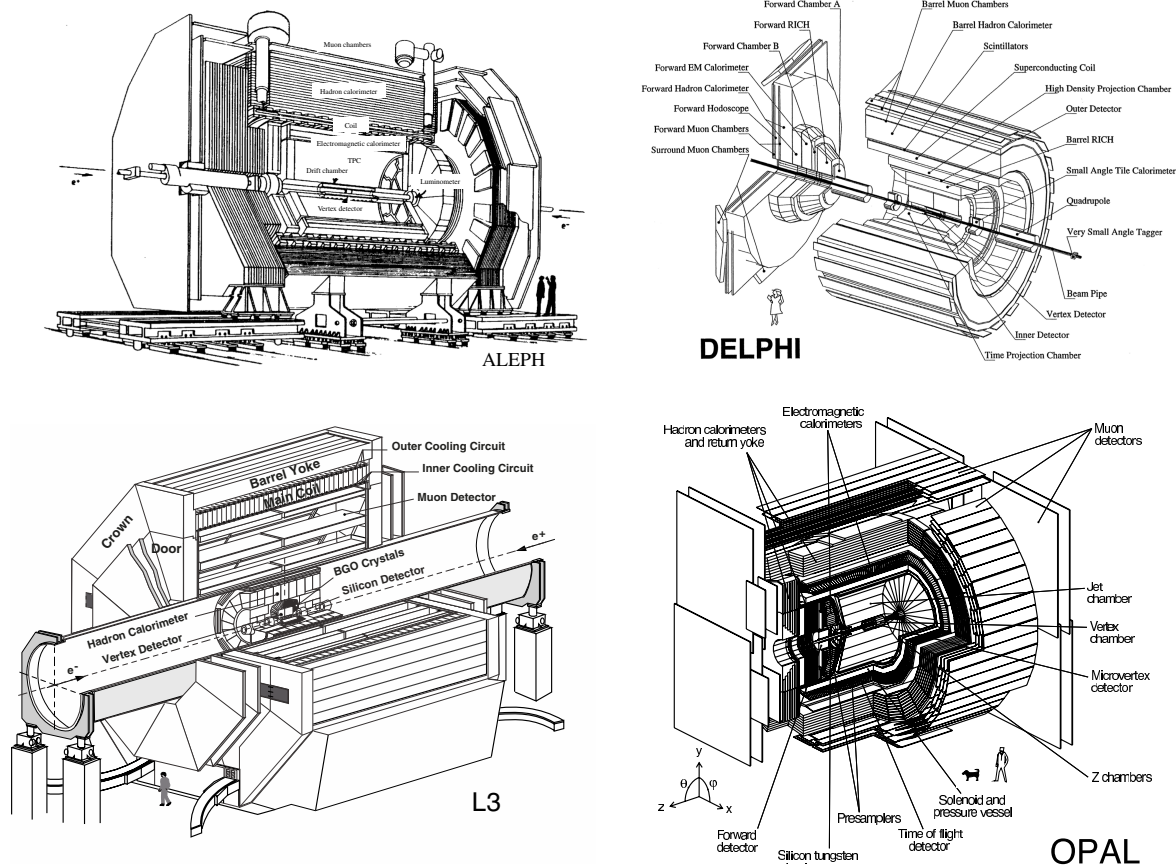


Fig. 2. Cut-away representation of the four LEP detectors: ALEPH, DELPHI, L3 and OPAL.

entire muon spectrometer is contained in the magnetic field. Some sub-detectors relied on established technology, such as wire chambers for tracking or crystals and scintillator counters for calorimetry, pushing technologies in scale and precision (e.g. the L3 BGO electromagnetic calorimeter, or its high-precision muon spectrometer). Other sub-detector relied on newer technologies, never deployed before on such a large scale (e.g. the ALEPH and DELPHI time-projection chambers, the ALEPH liquid-argon calorimeter and the DELPHI ring imaging Čerenkov detector — RICH).

Some examples of the performance of the LEP detectors are the following:

- the transverse momentum resolution of the ALEPH tracking system, $\sigma(1/p_t) = 0.6 \times 10^{-3} \text{ GeV}^{-1}$,¹⁹
- the DELPHI RICH efficiency of 70% to identify K^\pm with a contamination of 30%;²⁰
- the energy resolution of the L3 electromagnetic calorimeter $\Delta E/E \approx 1.4\%$ for 45 GeV electrons;²¹
- the momentum resolution of the L3 muon spectrometer $\Delta p/p \approx 2.5\%$ for 45 GeV muons.²¹

Figure 3 illustrates the detection principles for Z-boson decays. Hadronic events are identified from a high multiplicity of tracks in the central trackers and energy deposits in the calorimeters, reconstructed in two back-to-back fully-contained jets. Higher jet multiplicity is possible for rarer higher-order QCD processes. Z-boson decays in electron-positron pairs are characterised by two back-to-back tracks in the central trackers, corresponding to high-energy signals in the electromagnetic calorimeters. Z-boson decays into muons have the unique signature of back-to-back tracks in the central trackers, leaving minimum ionising deposits in the hadronic and electromagnetic calorimeters and tracks in the muon chambers. Z-boson decays in tau pairs are more challenging to detect, requiring a combination of missing energy in the detector, low-multiplicity jets, muons or electrons, according to the tau decay channels.

3.2. Data sample

The LEP accelerator operated at and around the Z-boson resonance from its commissioning in 1989 through 1995. In 1990 and 1991, energy scans at a spacing of 1 GeV provided a first mapping of the Z-boson resonance. In the following years, high-luminosity data-taking concentrated on the Z-boson resonance, with two additional “off-peak” energy points in 1993 and 1995, 1.8 GeV above and below the Z-boson resonance, to further constrain the Z-boson lineshape. Further details on the LEP accelerator design and performance are given in Ref. 22.

A total of 17 million Z-boson decays were detected by the four experiments. Table 2 provides a breakdown of the integrated luminosity per each experiment and the total number of events detected in the hadronic and leptonic final states.

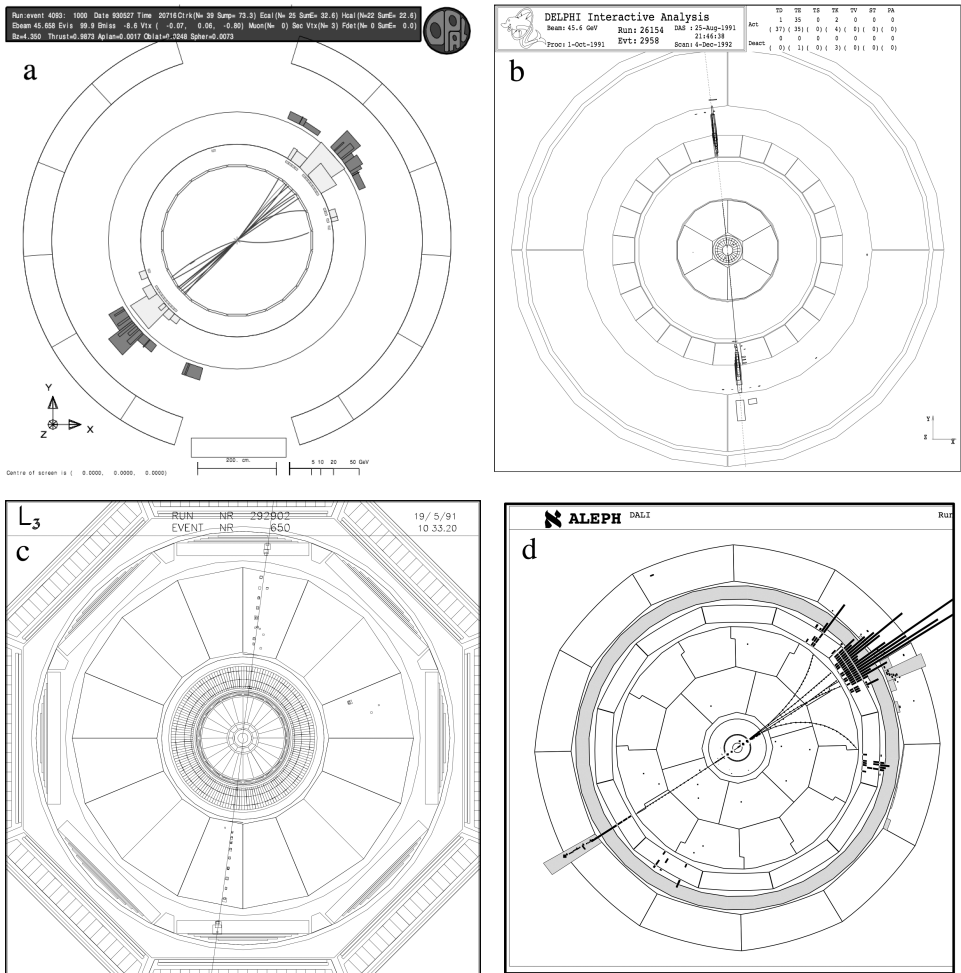


Fig. 3. Event displays of Z-boson decays detected in the four LEP experiments: (a) hadronic decays with the OPAL detector, characterised by two high-multiplicity back-to-back fully-contained jets; (b) electron-positron pairs with DELPHI, with two back-to-back tracks in the central tracker, and two energy deposits in the electromagnetic calorimeter, with energies close to the beam energy; (c) muon pairs with L3, with tracks in the muon chambers (mostly outside the image), minimum ionizing deposits in the hadronic and electromagnetic calorimeters and corresponding tracks in the central chambers, time-of-flight detectors assure such tracks are originating from the collision vertex and not from cosmic rays; (d) tau pairs with ALEPH, in this case with an electron (track and calorimeter deposit) detected in the hemisphere opposite a collimated, low-multiplicity jet, with overall missing energy. In all images the beam axis is perpendicular to the page.

Table 2 Centre-of-mass energy and luminosity delivered to each experiment, and total numbers of events collected by the four experiments in the hadronic and leptonic decay modes. Due to the low integrated luminosity and relative control of the experimental conditions, the 1989 data sample is not used in the study of the Z-boson lineshape.

Year	Centre-of-mass energy [GeV]	Integrated luminosity/experiment [pb^{-1}]	Total detected hadronic events [$\times 10^3$]	Total detected leptonic events [$\times 10^3$]
1990/91	88.2–94.2	27.5	1660	186
1992	91.3	28.6	2741	294
1993	89.4, 91.2, 93.0	40.0	2607	296
1994	91.2	64.5	5910	657
1995	89.4, 91.3, 93.0	39.8	2579	291

3.3. Measurement of cross-sections and asymmetries

In each final state of Z-boson decays, cross-sections are measured as $\sigma_{\text{tot}} = (N_s - N_b)/\varepsilon\mathcal{L}$, where N_s is the number of selected events, N_b is the number of events expected from background processes, ε is the selection efficiency, which include geometrical acceptance, and \mathcal{L} is the integrated luminosity. The LEP experiments derive N_b and ε from Monte Carlo generators describing the kinematics of both the Z-boson production and decay and of background processes. Events produced with those generators are passed through detailed simulations of the detectors and the same software used to reconstruct collision events. These workflows are cross-checked by using data and refined through the years to give extremely accurate simulation of the detectors.

Asymmetries for each final state are measured as $A_{\text{FB}} = (N_{\text{F}} - N_{\text{B}})/(N_{\text{F}} + N_{\text{B}})$, where N_{F} and N_{B} are event counts for negatively charged leptons ‘continuing’ along the direction of the incoming electron, or emitted ‘backwards’, respectively.

The large statistical sample of Z-boson decays collected at LEP results in low statistical uncertainties in the cross-section determinations for each experiment, around 0.5 per mille in the hadronic channel and 2.5 per mille in the leptonic channels. Experiment-dependent systematic uncertainties are mostly due to the calculation of efficiencies and acceptances and the selection procedures, as estimated from data and Monte Carlo simulations. These vary between 0.4 and 0.7 per mille in the hadronic channel and 1 to 7 per mille in the leptonic channel, with the higher value corresponding to tau pairs. For asymmetries, experiment-dependent systematic uncertainties have absolute values between 0.0005 and 0.0030, with the higher value corresponding to tau pairs. Statistical uncertainties are between two and five times larger than the systematic uncertainties.^{14, 23–26}

Systematic uncertainties on cross-sections and asymmetries which are common across experiments are irreducible. The main sources are: the LEP energy calibration;²² the use of the same Monte Carlo generators to simulate signal

and background processes; theoretical uncertainties on the parametrisation of Standard Model observables, contributions to the electron–positron final states, and the overall QED final-state corrections. The most important source of common systematical uncertainties affects the determination of luminosity, as discussed in the next section.

3.4. Measurement of luminosity

As presented in Eqs. (7) and (8), and in Fig. 1, N_ν depends strongly on the scale of the hadronic cross-section. As detectors are well understood and the large event counts limit statistical uncertainties, the N_ν precision depends on the accuracy of the luminosity measurement. LEP experiments relied on the detection of low-angle Bhabha scattering events for the measurement of instantaneous luminosity.²⁷ The advantages of this process is a high cross-section and therefore a negligible statistical uncertainty, as well as a low contribution from Z-boson production itself.

Pairs of dedicated calorimeters, completed with tracking devices, were installed close to the LEP beam pipe, in the forward and backward low-angle regions, typically between 30 and 50 mrad from the beam axis. Delicate to operate, these instruments had to be protected from hazardous conditions while beams were manipulated in the machine before stable collisions, and would then count coincidence of energy deposits in the forward and backward regions, originated by charged particles and compatible with the beam energy: the typical signature of Bhabha scattering. Event counts yield a detailed record of the instantaneous luminosity conditions and then allow to extract the total integrated luminosity. Experiment-dependent, systematic uncertainties for the determination of the luminosity are well controlled, in the range 0.03–0.09%.

All experiment relied on the same Monte Carlo generator and state-of-the-art theoretical calculations to estimate the accepted low-angle Bhabha scattering cross-section, and derive the luminosity.²⁸ After intense effort in improving these calculations, a residual theoretical uncertainty of 0.061% remains, mostly originating from vacuum polarisation, higher-order corrections and the production of light fermion pairs.²⁹ The way the luminosity uncertainty has been reduced over the LEP data-taking campaign tells a success story of highly sophisticated experimental techniques moving in lockstep with dedicated efforts by the theory community to push the understanding of the calculation of low-angle Bhabha scattering.

The LEP-wide combination of cross-sections and asymmetries, in addition to the obvious statistical advantages, allows to reduce several uncorrelated systematic uncertainties of experimental origin. At the same time, the theoretical uncertainty on the determination of the luminosity uncertainty is common to all experiments, and therefore irreducible. It contributes as much as a half of the uncertainty on the hadronic pole cross-section determination and dominates the systematic uncertainty on the determination of the N_ν , as discussed in the following sections.

3.5. Results

Each LEP experiment extracted cross-sections and asymmetries in the hadronic and leptonic final states at different energy points, corresponding to about 200 individual measurements. These allowed a precise description of the Z-boson lineshape and the corresponding extraction of parameters of the Standard Model.^{23–26}

An additional, through then unprecedented, collaborative efforts across the experiments led to the establishment of the LEP ElectroWeak Working Group.³⁰ The Group had the mandate to devise and arrange the combination of the Z-boson lineshape measurements across the experiments and thus obtain a considerable reduction of uncertainties, both of a statistical and systematic nature. Each experiment provided results in agreed-upon formats, with full correlation matrices. The LEP ElectroWeak Working Group combined¹⁴ all inputs to both determine the Z-boson lineshape observables with a much higher precision than allowed by each individual experiment statistical sample and check the overall consistency of the results and their implication for the understanding of the Standard Model.²² Table 3 presents combined results for the observables introduced in Section 2.2, in the hypothesis of lepton universality. The combination shows the compatibility of results across the experiments, with a goodness-of-fit of $\chi^2/\text{d.o.f.} = 36.5/31$.

It is important to remark that the lepton universality hypothesis is tested in the entire LEP data sample by measuring the ratios of the Z boson partial decay widths as $\Gamma_{\mu\mu}/\Gamma_{ee} = 1.0009 \pm 0.0028$ and $\Gamma_{\tau\tau}/\Gamma_{ee} = 1.0019 \pm 0.0032$.¹⁴

Using Eqs. (7) and (8) and the Standard Model value for the ratio of the Z-boson widths to neutrinos and leptons¹⁴

$$(\Gamma_{\nu\nu}/\Gamma_l)_{\text{SM}} = 1.99125 \pm 0.00083, \quad (9)$$

the number of light neutrino species is determined as:

$$N_\nu = 2.9840 \pm 0.0082. \quad (10)$$

It is important to recall the four key assumptions leading to this result:

- lepton universality holds;
- no other Z-boson decays exist beyond those to known fermions;

Table 3 Combined LEP results, and their correlation for key observables (Section 2.1).¹⁴

Observable	Combined LEP measurement	Correlations				
		m_z	Γ_z	σ_{had}^0	R_l^0	$A_{\text{FB}}^{0,1}$
m_z	$91.1875 \pm 0.021 \text{ GeV}$	1.000				
Γ_z	$2.4952 \pm 0.0023 \text{ GeV}$	-0.023	1.000			
σ_{had}^0	$41.540 \pm 0.037 \text{ nb}$	-0.045	-0.297	1.000		
R_l^0	20.767 ± 0.025	0.033	0.004	0.183	1.000	
$A_{\text{FB}}^{0,1}$	0.0171 ± 0.0010	0.055	0.033	0.006	-0.056	1.000

- neutrino masses are negligible;
- Z-boson couplings to neutrinos are described by the Standard Model.

3.6. Uncertainties

The uncertainty on N_ν is less the three per mille. It is decomposed as the sum in quadrature of three parts:¹⁴

$$\delta N_\nu \sim 10.5 \frac{\delta n_{\text{had}}}{n_{\text{had}}} \oplus 3.0 \frac{\delta n_{\text{lep}}}{n_{\text{lep}}} \oplus 7.5 \frac{\delta \mathcal{L}}{\mathcal{L}}. \quad (11)$$

The first two are related to uncertainties on the number of events selected for the measurement of cross-section and asymmetries in the hadronic and leptonic channels, respectively. The third term parametrises uncertainties on the scale of the cross-sections deriving from the uncertainties on the luminosity measurement.

The largest contribution to the uncertainty on the luminosity measurement is the theoretical uncertainty (0.061%) discussed in Section 3.4. This uncertainty alone results in an uncertainty on N_ν of 0.0046, accounting for more than half of the total uncertainty on N_ν .

4. Direct Measurement of N_ν

The LEP experiments pursued an alternative and elegant measurement of N_ν by detecting events with a single visible photon as a signature of the $e^-e^+ \rightarrow \nu\bar{\nu}\gamma$ process.² At the Z-boson resonance, this final state is mostly due to the initial-state radiation of a low-angle photon, with a steeply falling energy spectrum, with a Z boson decaying into neutrinos. Contributions from the t-channel exchange of a virtual W boson are small.

At the Z-boson resonance, the cross-section of the $e^-e^+ \rightarrow \nu\bar{\nu}\gamma$ process can be written³¹ as

$$\sigma_{\nu\bar{\nu}\gamma}^0(s) = \frac{12\pi}{m_Z^2} \frac{s\Gamma_{ee}N_\nu\Gamma_{\nu\nu}}{(s - m_Z^2) + s^2\Gamma_Z^2/m_Z^2} + \text{W-boson exchange terms} \quad (12)$$

which is mostly proportional to N_ν . A careful measurement of the cross-section of the process with the control of the residual background sources and the overall acceptance allows to extract N_ν . This cross-section is considerably lower than the Z-boson resonance. The statistical accuracy of the direct measurement of N_ν is therefore over an order of magnitude inferior than the indirect measurement. At the same time, the direct measurement does not rely on the assumption that Z bosons only decay to known fermions. Possible decays into visible ‘exotic’ particles, conflated within other visible channels and in particular hadronic final states, could in principle alter the Z-boson lineshape and yield an incorrect measurement of N_ν .

The key experimental challenge of the direct measurement is to detect events with a single photon and no other activity in the detector. On the one hand, the

cross-section is larger, and therefore the measurement more sensitive, the lower the energy of the photon and the closest the photon is to the beam axis. On the other hand, these exact conditions make both photon detection more complex and experimental backgrounds harder to control. The four LEP experiments devised sophisticated analysis chains and in some cases even dedicated trigger systems to record these “single photon” events (e.g. the one described in Ref. 32). Around 2500 single photon events, with background subtracted, were collectively detected by the four experiments at the Z-boson resonance, with different energy thresholds and fiducial volumes, as summarised in Table 4, which also details data samples and the signal-over-background ratios.

Figure 4 presents an example of the measured cross-section as a function of the centre-of-mass energy and its dependency on N_ν . Fits to the theoretical modeling of the cross-section, with the assumption of Standard Model coupling of the Z-boson to neutrinos, yield the individual direct measurements of N_ν listed in Table 4. These results can be combined as³⁷:

$$N_\nu = 3.00 \pm 0.08. \tag{13}$$

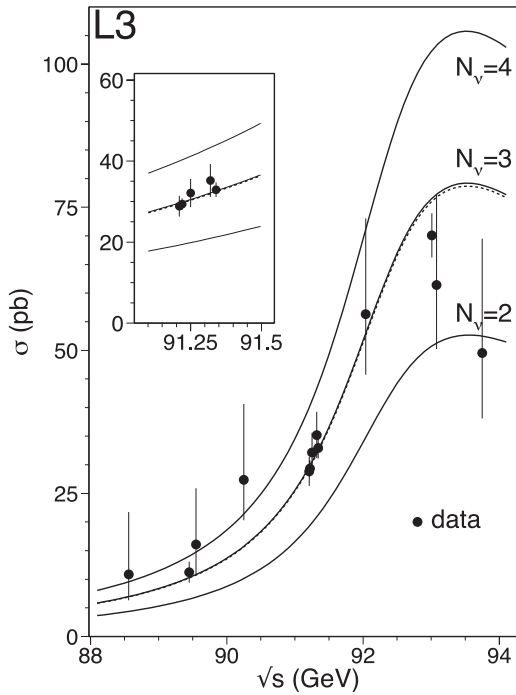


Fig. 4. Cross-section measured by the L3 experiment for the $e^-e^+ \rightarrow \nu\bar{\nu}\gamma$ process around the Z-boson resonance as a function of the centre-of-mass energy. The lower limit for the photon energy is 1 GeV, and the fiducial volume $|\cos\theta_\gamma| < 0.71$. Theoretical predictions for two, three or four light neutrinos species are also shown. The dashed line represents a fit to the data points.³⁵

Table 4 Integrated luminosity, \mathcal{L} , photon energy threshold, E_γ , and fiducial volume, $|\cos\theta_\gamma|$, for the four LEP experiments' analyses of single-photon events around the Z-boson resonance. The signal over background ratios, s/b, are also given, together with each experiment direct measurement of N_ν and their average. The first uncertainties are statistical and the second systematic.

Experiment	\mathcal{L} [pb $^{-1}$]	$E_\gamma >$ [GeV]	$ \cos\theta_\gamma <$	s/b	N_ν	Reference
ALEPH	15.7	1.5	0.74	1.8	$2.68 \pm 0.20 \pm 0.20$	33
DELPHI	67.6	3.0	0.70	2.7	$2.89 \pm 0.32 \pm 0.19$	34
L3	99.9	1.0	0.71	6.0	$2.98 \pm 0.07 \pm 0.07$	35
OPAL	40.5	1.75	0.70	11.0	$3.23 \pm 0.16 \pm 0.10$	36
Average					3.00 ± 0.08	37

Table 5 Direct measurement of N_ν at centre-of-mass energies, \sqrt{s} , above the Z-boson resonance. Each experiments investigated different observables to extract N_ν .

Experiment	\sqrt{s} [GeV]	Observable(s)	N_ν	Reference
ALEPH	189–207	Missing mass, θ_γ	2.86 ± 0.09 (stat.+syst.)	41
DELPHI	130–209	Cross section	2.84 ± 0.10 (stat.) ± 0.14 (syst.)	42
L3	130–209	Recoil mass, θ_γ	2.95 ± 0.08 (stat.) ± 0.03 (syst.) ± 0.03 (th.)	43
OPAL	130–189	E_γ	3.27 ± 0.30 (stat.+syst.)	44
Average (including lower energies)			2.92 ± 0.05	37

The LEP experiments repeated this measurements at centre-of-mass energies above the Z-boson resonance. At these higher energies, from 130 GeV to 209 GeV, the single-photon energy spectrum exhibits two distinct features. The first feature is a steeply falling behavior similar to that observed at the Z-boson resonance, mostly due to the initial-state radiation of a photon accompanying the t-channel production of a neutrino–antineutrino pair through the exchange of a virtual W boson. The second feature is a peak at the energy corresponding to the difference between the centre-of-mass energy and the Z-boson mass. This structure corresponds to the radiation in the initial state of a photon of the energy needed to lower the centre-of-mass energy back to the Z-boson resonance, with a Z boson decaying into neutrinos. Monte Carlo simulations of these processes^{38–40} allow to model the dependence of the photon energy spectrum, and its polar angle, on N_ν .

The four experiments collectively detected about 6200 single photon events above the Z-boson resonance, with relatively low background. The study of various observables allows to extract N_ν , with the results summarised in Table 5. Including lower-energy data, the combined result for the direct determination of the number of light neutrino species across all LEP energies is:³⁷

$$N_\nu = 2.92 \pm 0.05. \quad (14)$$

5. Conclusions

In 1989, within the first few weeks of data taking at LEP, the ALEPH, DELPHI, L3 and OPAL collaborations reported the number of light neutrino species to be around three. This is a remarkable achievement which bears witness to the performance of the LEP accelerator, the early understanding of detectors, and the overall planning of the LEP physics program: the most complex CERN had seen in its first four decades. It would take five more years of data-taking, and about a decade more to develop sophisticated analysis techniques to combine results across the LEP experiments, for the final determination of the number of light neutrino species to be published as:¹⁴

$$N_\nu = 2.9840 \pm 0.0082.$$

The dominating uncertainty is the theoretical control of the low-angle Bhabha scattering process used to determine the experimental luminosity. This result relies on four important assumptions: that lepton universality holds; that Z bosons only decay to known fermions; that neutrino masses are negligible; and finally that Z-boson couplings to neutrinos are as described by the Standard Model. The direct measurement of the $e^-e^+ \rightarrow \nu\bar{\nu}\gamma$ process, at the Z-boson resonance and at higher centre-of-mass energies up to 209 GeV, allows an independent verification, obtaining a value $N_\nu = 2.92 \pm 0.05$.

This result stands out as one of the legacies of the LEP physics program. It ruled out for the first time the existence of a fourth generation, and poses stringent limits on theoretical models relevant in astrophysics and cosmology. The high precision of the result further constrains the existence of exotic particles in Z-boson decays. Beyond the tremendous physical importance, the impressive precision of the measurement of the number of light neutrino species at LEP, and the overall determination of the parameters of the Standard Model and the proof of its internal consistency,²² mark a turning point in the history of CERN as an example of scientific cooperation.

The LEP detectors were the first to be built by truly worldwide collaborations, with large contingents of scientists from the United States and Asia participating to a CERN program. Unprecedented in size, the LEP collaborations were the mold for the true globalisation of particle physics as an enterprise, and of CERN as a laboratory, which ushered the LHC era over the two most recent decades in CERN's history. This example of global scientific collaboration has captured worldwide attention, and imagination, at the time of the first LHC discoveries. It is more than an anecdote, but rather a proof of how scientific cooperation is indispensable to extend human knowledge, that the scientific publication describing the high-precision measurements at LEP¹⁴ was signed by over 2500 authors, the first ever published article to do so.^b

^bContrary to what is sometimes heard, the first published article with more than 1000 authors is not on high-energy physics, but about a large-scale Japanese medical study.^{45, 46}

The LEP era transformed CERN, with large and crucial contributions from scientists of the then Soviet Union and countries from Eastern Europe, alongside scientists from the United States and Western Europe. This process enshrined the crucial role of CERN as an ambassador of ‘Science for Peace’, recently recognised by the United Nations in granting CERN observer status at its General Assembly.

On the one hand, the precise determination of the number of light neutrino species is of fundamental importance for our understanding of the Universe. On the other hand, the decade-long global cooperative effort to achieve this result, through the ingenuity and creativity of thousands of dedicated individuals, is part of our collective legacy as the human species.

References

1. H. Schopper, *LEP — The Lord of the Collider Rings at CERN* (Springer, 2009).
2. G. Barbiellini *et al.*, Neutrino counting, in *Proceedings of the Workshop on Z Physics at LEP*, CERN, Switzerland (Sept. 1989), pp. 129–170.
3. C. Rubbia, The discovery of the W and Z particles, in *60 Years of CERN Experiments and Discoveries*. (World Scientific, 2015).
4. D. Decamp *et al.* (ALEPH Collaboration), A precise determination of the number of families with light neutrinos and of the z-boson partial widths, *Phys. Lett. B* **231**, 519–529 (1989).
5. P. Aarnio *et al.* (DELPHI Collaboration), Measurement of the mass and width of the Z^0 -particle from multihadronic final states produced in e^+e^- annihilations, *Phys. Lett. B* **231**, 539–547 (1989).
6. B. Adeva *et al.* (L3 Collaboration), A determination of the properties of the neutral intermediate vector boson Z^0 , *Phys. Lett. B* **231**, 509–518 (1989).
7. M. Z. Akrawy *et al.* (OPAL Collaboration), A precise determination of the number of families with light neutrinos and of the Z-boson partial widths, *Phys. Lett. B* **231**, 530–538 (1989).
8. J. J. Hernandez *et al.* (Particle Data Group), Review of particle properties, *Phys. Lett. B* **239**, VI.22–VI.23 (1990).
9. K. Chetyrkin *et al.*, QCD corrections to the e^+e^- cross section and the Z-boson decay rate. In *Reports of the working group on precision calculations for the Z resonance*, CERN, Switzerland (Mar. 1993), pp. 175–264.
10. A. Czarnecki and J. Kuhn, Nonfactorizable QCD and electroweak corrections to the hadronic Z boson decay rate, *Phys. Rev. Lett.* **77**, 3955–3958 (1996).
11. R. Harlander *et al.*, Complete corrections of $O(\alpha_s)$ to the decay of the Z-boson into bottom quarks, *Phys. Lett. B* **426**, 125–132 (1998).
12. K. Olive *et al.* (Particle Data Group), Review of Particle Physics, *Chin. Phys. C* **38**, i–1676 (2014).
13. M. Veltman, Limit on Mass Differences in the Weinberg Model, *Nucl. Phys. B* **123**, 89–99 (1977).
14. S. Schael *et al.* (ALEPH, DELPHI, L3, OPAL and SLD Collaborations and the LEP Electroweak Working Group, SLD Electroweak Group and SLD Heavy Flavour

- Group Collaborations), Precision electroweak measurements on the Z Resonance, *Phys. Rept.* **427**, 257–454 (2006).
15. D. Decamp *et al.* (ALEPH Collaboration), ALEPH: A detector for electron-positron annihilations at LEP, *Nucl. Instrum. Meth. A* **294**, 121–178 (1990).
 16. P. Aarnio *et al.* (DELPHI Collaboration), The DELPHI detector at LEP, *Nucl. Instrum. Meth. A* **303**, 233–276 (1991).
 17. B. Adeva *et al.* (L3 Collaboration), The construction of the L3 experiment, *Nucl. Instrum. Meth. A* **289**, 35–102 (1990).
 18. K. Ahmet *et al.* (OPAL Collaboration), The OPAL detector at LEP, *Nucl. Instrum. Meth. A* **303**, 275–319 (1991).
 19. D. Busculic *et al.* (ALEPH Collaboration), Performance of the ALEPH detector at LEP, *Nucl. Instrum. Meth. A* **360**, 481–506 (1995).
 20. P. Abreu *et al.* (DELPHI Collaboration), Performance of the DELPHI detector, *Nucl. Instrum. Meth. A* **378**, 57–100 (1996).
 21. O. Adriani *et al.* (L3 Collaboration), Results from the L3 experiment at LEP, *Phys. Rept.* **236**, 1–146 (1993).
 22. W. de Boer, Precision Experiments at LEP, in *60 Years of CERN Experiments and Discovery* (World Scientific, 2015).
 23. R. Barate *et al.* (ALEPH Collaboration), Measurement of the Z resonance parameters at LEP, *Eur. Phys. J. C* **14**, 1–50 (2000).
 24. P. Abreu *et al.* (DELPHI Collaboration), Cross-sections and leptonic forward backward asymmetries from the Z0 running of LEP, *Eur. Phys. J. C* **16**, 371–405 (2000).
 25. M. Acciarri *et al.* (L3 Collaboration), Measurements of cross-sections and forward backward asymmetries at the Z resonance and determination of electroweak parameters, *Eur. Phys. J. C* **16**, 1–40 (2000).
 26. G. Abbiendi *et al.* (OPAL Collaboration), Precise determination of the Z resonance parameters at LEP: ‘Zedometry’, *Eur. Phys. J. C* **19**, 587–651 (2001).
 27. G. M. Dallavalle, Review of precision determinations of the accelerator luminosity in LEP experiments, *Acta Phys. Pol. B* **28**, 901–923 (1997).
 28. S. Jadach *et al.*, Upgrade of the Monte Carlo program BHLUMI for Bhabha scattering at low angles to version 4.04, *Comput. Phys. Commun.* **102**, 229–251 (1997).
 29. B. Ward *et al.*, New results on the theoretical precision of the LEP/SLC luminosity, *Phys. Lett. B* **450**, 262–266 (1999).
 30. LEP Electroweak Working Group, <http://lepewwg.web.cern.ch/LEPEWWG/>, last accessed February 6th, 2015.
 31. O. Nicosini and L. Trentadue, Structure Function Approach to the Neutrino Counting Problem, *Nucl. Phys. B* **318**, 1–21 (1989).
 32. R. Bizarri *et al.*, The First level energy trigger of the L3 experiment: Description of the hardware, *Nucl. Instrum. Meth. A* **317**, 463–473 (1992).
 33. D. Buskulic *et al.* (ALEPH Collaboration), A Direct measurement of the invisible width of the Z from single photon counting, *Phys. Lett. B* **314**, 520–534 (1993).
 34. P. Abreu *et al.* (DELPHI Collaboration), Search for new phenomena using single photon events in the DELPHI detector at LEP, *Z. Phys. C* **74**, 577–586 (1997).

35. M. Acciarri *et al.* (L3 Collaboration), Determination of the number of light neutrino species from single photon production at LEP, *Phys. Lett. B* **431**, 199–208 (1998).
36. R. Akers *et al.* (OPAL Collaboration), Measurement of single photon production in e^+e^- collisions near the Z^0 resonance, *Z. Phys. C* **65**, 47–66 (1995).
37. C. Amsler *et al.* (Particle Data Group), Review of Particle Physics, *Phys. Lett. B* **667**, 1–1340 (2008).
38. S. Jadach *et al.*, The Precision Monte Carlo event generator KK for two fermion final states in e^+e^- collisions, *Comput. Phys. Commun.* **130**, 260–325 (2000).
39. S. Jadach *et al.*, The Monte Carlo program KORALZ, version 4.0, for the lepton or quark pair production at LEP / SLC energies, *Comput. Phys. Commun.* **79**, 503–522 (1994).
40. G. Montagna *et al.*, Single photon and multiphoton final states with missing energy at e^+e^- colliders, *Nucl. Phys. B* **541**, 31–49 (1999).
41. A. Heister *et al.* (ALEPH Collaboration), Single photon and multiphoton production in e^+e^- collisions at \sqrt{s} up to 209 GeV, *Eur. Phys. J. C* **28**, 1–13 (2003).
42. J. Abdallah *et al.* (DELPHI Collaboration), Photon events with missing energy in e^+e^- collisions at $\sqrt{s} = 130$ GeV to 209 GeV, *Eur. Phys. J. C* **38**, 395–411 (2005).
43. P. Achard *et al.* (L3 Collaboration), Single photon and multiphoton events with missing energy in e^+e^- collisions at LEP, *Phys. Lett. B* **587**, 16–32 (2004).
44. G. Abbiendi *et al.* (OPAL Collaboration), Photonic events with missing energy in e^+e^- collisions at $\sqrt{s} = 189$ GeV, *Eur. Phys. J. C* **18**, 253–272 (2000).
45. C. King, Multiauthor Papers: Onward and Upward, in *ScienceWatch Newsletter*, July 2012, http://archive.sciencewatch.com/newsletter/2012/201207/multiauthor_papers, last accessed February 6th, 2015.
46. H. Nakamura, *et al.* (MEGA Study Group), Design and baseline characteristics of a study of primary prevention of coronary events with pravastatin among Japanese with mildly elevated cholesterol levels, *Circulation J.* **68**, 860–7 (2004).